Spectrochimica Acta Part A: Molecular and Biomolecular Spectroscopy 138 (2015) 58–66

Contents lists available at ScienceDirect

Spectrochimica Acta Part A: Molecular and Biomolecular Spectroscopy

journal homepage: www.elsevier.com/locate/saa

Synthesis, spectroscopic characterization and pH dependent photometric and electrochemical fate of Schiff bases

Abdur Rauf [a], Afzal Shah [a,b,*], Saghir Abbas [a], Usman Ali Rana [c], Salah Ud-Din Khan [c], Saqib Ali [a], Zia-ur-Rehman [a], Rumana Qureshi [a], Heinz-Bernhard Kraatz [b], Francine Belanger-Gariepy [d]

[a] Department of Chemistry, Quaid-i-Azam University, 45320 Islamabad, Pakistan
[b] Department of Physical and Environmental Sciences, University of Toronto Scarborough, 1265 Military Trail, Toronto M1C 1A4, Canada
[c] Deanship of Scientific Research, College of Engineering, King Saud University, Riyadh 11421, Saudi Arabia
[d] Department de Chimie, Universite de Montreal, Montreal, Canada

HIGHLIGHTS

- Two Schiff bases were successfully synthesized by a facile approach.
- These were characterized by ^{1}H NMR, ^{13}C NMR, FTIR and UV–Vis spectroscopy.
- The pH dependent redox and photometric behavior was investigated in a wide pH range.
- The experimental findings were supported by quantum mechanical approach.
- Isosbestic points indicated the existence of Schiff bases in different tautomeric forms.

GRAPHICAL ABSTRACT

Two Schiff bases were synthesized and characterized. Their pH dependent spectroscopic and electrochemical behavior was investigated. They were found as good ligands and inhibitors of alkaline phosphatase.

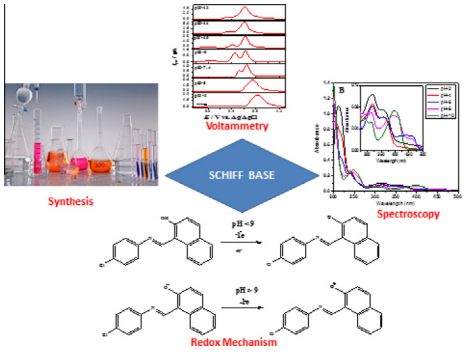

ARTICLE INFO

Article history:
Received 30 July 2014
Received in revised form 14 October 2014
Accepted 23 October 2014
Available online 15 November 2014

Keywords:
Schiff base
Spectroscopic characterization
Isosbestic point
Redox mechanism

ABSTRACT

A new Schiff base, 1-((4-bromophenylimino) methyl) naphthalen-2-ol (BPIMN) was successfully synthesized and characterized by ^{1}H NMR, ^{13}C NMR, FTIR and UV–Vis spectroscopy. The results were compared with a structurally related Schiff base, 1-((4-chlorophenylimino) methyl) naphthalen-2-ol (CPIMN). The photometric and electrochemical fate of BPIMN and CPIMN was investigated in a wide pH range. The experimental findings were supported by quantum mechanical approach. The redox mechanistic pathways were proposed on the basis of results obtained electrochemical techniques. Moreover, pH dependent UV–Vis spectroscopy of BPIMN and CPIMN was carried out and the appearance of isosbestic points indicated the existence of these compounds in different tautomeric forms.

Introduction

Schiff bases have been reported to form metal complexes of wide biological applications due to their stability in different oxidation states [1,2]. These compounds are bestowed with good anticancer, antibacterial, antifungal, and herbicidal activities [3–5]. Thus, spurred on by the broad range applications of Schiff bases, the synthesis of new chemotherapeutic candidates of this

* Corresponding author at: Department of Chemistry, Quaid-i-Azam University, 45320 Islamabad, Pakistan. Tel.: +92 416 208 2776.
E-mail addresses: afzal.shah@utoronto.ca, afzals_qau@yahoo.com (A. Shah).

http://dx.doi.org/10.1016/j.saa.2014.10.111
1386-1425/

class is the prime objective of medicinal chemists [6]. Some of their derivatives from various amine and carbonyl derivatives have been reported to possess genotoxicity and antimicrobial activities [7,8]. Schiff bases containing hydroxyl group have received the utmost attention of chemists and physicists due to their special photochromic/thermochromic characteristics and electrochemical applications [9–11]. These pH dependent proton exchanging compounds are also applied in the designing of different molecular electronic devices [12]. Moreover, hydroxyl-substituted Schiff bases possess antioxidant activities [13]. Metal complexes of these bases are also fascinating due to their environmental importance [14,15]. Some Schiff bases have been documented to protect metals from aggressive medium by adsorption at metals surfaces [16–18]. Based on these considerations we synthesized a new Schiff base, 1-((4-bromophenylimino) methyl) naphthalen-2-ol (BPIMN) and characterized by a variety of techniques.

Schiff bases find use as catalyst for oxygenation, hydrolysis, electro-reduction and decomposition of various compounds. The electrochemical study is envisioned to provide highly valuable information about the catalytic processes since catalytic conversions are frequently accompanied by change in oxidation state of the central metal and structure of the complex. Knowledge of electronic and steric effects to control the redox chemistry of these metal complexes may prove critical in the design of new catalysts [19,20]. As Schiff bases are highly biologically active compounds, so pH dependent photometric and voltammetric studies of two unexplored derivatives of this class were carried out getting useful insights about their role in cellular milieu.

Experimental

Chemicals

2-Hydroxy-1-naphthaldehyde, 4-bromoaniline and 4-chloroaniline were purchased from Aldrich, USA. The solvents like toluene, chloroform, hexane and ethanol were obtained from Merck, Germany and dried before use by following the standard reported procedures. *p*-Nitrophenyl phosphate hexahydrate, diethanolamine and magnesium chloride were purchased from Sigma Aldrich and used as received. Human serum was used as a source of alkaline phosphatase.

Instrumentation

Melting points were determined using Gallen Kamp apparatus. Infrared measurements (4000–400 cm^{-1}) were performed on thermoscientific NICOLET 6700 FTIR spectrophotometer. Multinuclear (^1H and ^{13}C NMR) spectra were recorded in solution on Bruker ARX 300 MHz using tetramethylsilane (TMS) as internal reference. UV–Visible 1601 Shimadzu spectrophotometer with measurement wavelength range of 200–800 nm was used for electronic absorption studies. Briton Robinson (BR) universal buffer of wide pH range was used for studying the effect pH on the photometric and voltammetric response of the analytes. The electrochemical studies were carried out in nitrogen saturated solutions using μAutolab running with GPES 4.9 software, Eco-Chemie, the Netherlands. A glassy carbon electrode (GCE) with electro-sensing area of 0.063 cm^2 was used as working electrode. Ag/AgCl (3 M KCl) and platinum wire were used as reference and counter electrodes. The electrode surface was polished by 0.3 μm alumina powder followed by thorough rinsing with bidistillated water. Stock solutions (2 mM) of BPIMN and CPIMN were prepared in analytical grade ethanol. Fresh working solutions were prepared in 50% ethanol and 50% BRB as supporting electrolyte. For reproducible experimental results, the clean GC electrode was used to place in supporting electrolyte solution and various cyclic voltammograms were recorded until the achievement of a steady state baseline voltammogram. Differential pulse voltammetry (DPV) was carried out at a scan rate of 5 mV s^{-1}. For square wave voltammetry, a scan rate of 100 mV s^{-1} was fixed by setting 20 Hz frequency and 5 mV potential increments. For computational studies, GAUSSIAN 03W package was used. The geometric optimization of BPIMN and CPIMN was done by density functional theory at B3LYP and 3-21G minimal bases set. The most stable conformation was used for the measurement of charge distribution and energy calculations of HOMO and LUMO. The reason for the selection of DFT/3-21G was its success in charge and energy calculations as testified by other investigators [21].

Synthesis of 1-((4-bromophenylimino) methyl) naphthalen-2-ol

The novel Schiff base was synthesized by reacting 2-hydroxynaphthaldehyde (0.03 mmol, 5.0 mg) and 4-chloroaniline (0.03 mmol, 5.16 mg) in dry ethanol (Scheme 1). The obtained yellow crystalline solid was cooled, filtered and recrystallized in mixture of chloroform and pet ether (3:1). The formation of BPIMN was ensured from the following data:

$C_{17}H_{12}NOBr$: Yield 75%, M.p. 162.5–164 °C, FT-IR (cm^{-1}): 1615.6 ν(C=N), 3387 $\nu(OH)_{phenolic}$, ^1H NMR δ (ppm): 9.15 {1H, CH=N}, 15.05 {1H, OH}, ^{13}C NMR δ (ppm): 168.6 {CH=N}, 155.7 {C-OH}.

Synthesis of 1-((4-chlorophenylimino) methyl) naphthalen-2-ol

The Schiff base ligand, abbreviated as CPIMN was synthesized and recrystallized by the method reported in literature [22]. The yield and spectroscopic data of CPIMN are given below:

$C_{17}H_{12}NOCl$: Yield 75%, M.p. 157–160 °C, FT-IR (cm^{-1}): 1620 ν(C=N), 3399 $\nu(OH)_{phenolic}$, ^1H NMR δ (ppm): 9.40 {1H, CH=N}, 15.25 {1H, OH}, ^{13}C NMR δ (ppm): 168.5 {CH=N}, 155.8 {C-OH}.

X-ray structure determination

Suitable single crystals of BPIMN and CPIMN were selected and mounted on a Microstar diffractometer. The crystal was kept at 100 K during data collection. The structure was solved with the olex2 using Charge Flipping program [23] and refined with XL

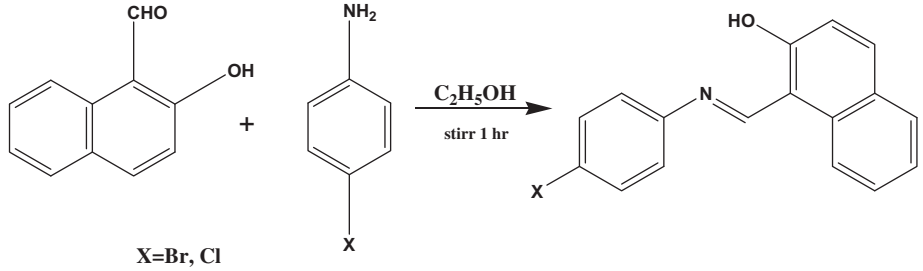

Scheme 1. Synthesis of 1-((4-bromophenylimino) methyl) naphthalen-2-ol and 1-((4-chlorophenylimino)methyl)naphthalen-2-ol.

[24] refinement package using least squares minimization. Crystal data and details of the parameters are summarized in Tables 1–3.

Assay of alkaline phosphatase activity

For alkaline phosphatase activity of the synthesized Schiff bases, the reported method [25] with slight modification was used. Working substrate was made by mixing four parts of reagent A (ethanolamine pH 9.8 mol/dm^3 and Magnesium chloride 0.5 mmol/dm^3) and one part of reagent B (*p*-nitrophenyl phosphate 50 mmol/dm^3). Substrate was incubated for 5 min at 25 °C. A 2 mL of the substrate was taken in a cuvette and 40 μL of human serum having activity of 165 IU/L was added. After incubation for 1 min, absorbance was measured to check the activity of enzyme. ALP hydrolyzed *p*-NPP and produced a yellow colored *p*-nitrophenol that showed absorbance at 405 nm (Scheme 2). After that various amounts of Schiff bases (20 μL, 40 μL, 60 μL) were periodically added from 6.25 mmolar stock solution and again incubated for 3 min. Absorbance was recorded after 1–5 min and in the end %age inhibition was calculated from the average.

Table 1
Crystal data and details of the structure refinement for BPIMN and CPIMN.

Structure refinements	BPIMN	CPIMN
Empirical formula	$C_{17}H_{12}NOBr$	$C_{17}H_{12}NOCl$
Formula weight	326.19	281.73
Temperature (K)	100	100
Crystal system	Monoclinic	Monoclinic
Space group	$P2_1/n$	$P2_1/n$
a (Å)	4.7671(3)	4.7136(6)
b (Å)	20.5291(11)	20.3076(18)
c (Å)	13.5235(7)	13.5174(18)
α (°)	90	90
β (°)	93.808(3)	93.830(8)
γ (°)	90	90
Volume (Å^3)	1320.55(13)	1291.0(3)
Z	4	4
ρ_{calc} (mg/mm^3)	1.641	1.449
m (mm^{-1})	4.184	2.557
F(000)	656.0	584.0
Crystal size (mm^3)	0.2 × 0.05 × 0.03	0.2 × 0.05 × 0.05
2Θ range for data collection	7.84–140.572°	7.868–139.968°
Index ranges	$-5 \leqslant h \leqslant 4$, $-24 \leqslant k \leqslant 24$, $-16 \leqslant l \leqslant 16$	$-4 \leqslant h \leqslant 5$, $-24 \leqslant k \leqslant 24$, $-13 \leqslant l \leqslant 11$
Reflections collected	26,005	4152
Independent reflections	2505[*R*(int) = 0.0696]	1721[*R*(int) = 0.0493]
Data/restraints/parameters	2505/2/189	1721/0/184
Goodness-of-fit on F^2	1.044	1.045
Final *R* indexes [$I \geqslant 2\sigma(I)$]	R_1 = 0.0331, wR_2 = 0.0885	R_1 = 0.0480, wR_2 = 0.1319
Final *R* indexes [all data]	R_1 = 0.0359, wR_2 = 0.0908	R_1 = 0.0544, wR_2 = 0.1382
Largest diff. peak/hole (e Å^{-3})	0.97/−0.67	0.34/−0.44

Results and discussion

Structural characterization

FT-IR spectrum of the newly synthesized Schiff base, BPIMN, showed a strong absorption band around 1734 cm^{-1} due to azomethine group. The appearance of proton resonance signal of CH=N at 9.15 ppm in the ^{1}H NMR spectrum confirmed the formation of Schiff base. The absence of any resonance peak corresponding to primary amine supported the purity of the product i.e. Schiff base. The characteristic resonance signal of CH=N at 168.63 in the ^{13}C NMR spectrum also verified the formation of the product.

Crystal structures description

The molecular structures of BPIMN and CPIMN along with crystallographic numbering schemes are shown in Fig. 1. Summary of crystal data and details of structural refinements can be seen in Table 1. Selected bond distances and bond angles of BPIMN and CPIMN are listed in Table 2. It is evident from the data that

Table 3
Hydrogen-bonding geometry (Å, °) for crystal BPIMN.

D	H	A	d(D—H) (Å)	d(H—A) (Å)	d(D—A) (Å)	D—H—A (°)
O1	H1	N1	0.83	1.79	2.516(3)	145
N1	H1A	O1	0.87	1.79	2.516(3)	140

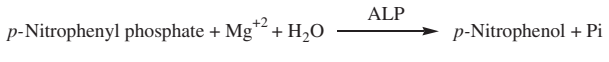

Pi denotes inorganic phosphate

Scheme 2. Hydrolysis of alkaline phosphatase.

Table 2
Selected experimental and calculated geometric parameters for BPIMN and CPIMN.

			BPIMN exp.	BPIMN calc.	Δ	CPIMN exp.	CPIMN calc.	Δ
Bond distance (Å)								
O1	C2		1.308(3)	1.386	0.078	1.305(3)	1.385	0.080
N1	C11		1.304(3)	1.293	−0.011	1.308(3)	1.293	−0.015
N1	C12		1.412(3)	1.416	0.004	1.411(4)	1.416	0.005
C1	C2		1.418(3)	1.399	−0.019	1.419(4)	1.400	−0.019
C1	C10		1.447(3)	1.443	−0.004	1.446(3)	1.443	−0.003
C1	C11		1.423(3)	1.461	0.038	1.419(4)	1.460	0.041
C15	X		1.900(2)	1.931	0.031	1.750(3)	1.834	0.084
Bond angles (°)								
C11	N1	C12	124.0(2)	120.8	−3.2	124.1(3)	120.8	−3.3
C2	C1	C10	119.9(2)	118.8	−1.1	119.9(2)	118.8	−1.1
C2	C1	C11	118.6(2)	115.8	−2.8	118.6(2)	115.8	−2.8
C11	C1	C10	121.6(2)	125.4	3.8	121.5(3)	125.4	3.9
O1	C2	C1	122.5(2)	118.0	−4.5	122.2(2)	118.0	−4.2
O1	C2	C3	118.1(2)	120.7	2.6	118.5(3)	120.7	2.2
N1	C11	C1	122.1(2)	125.6	3.5	122.1(3)	125.6	3.5
C13	C12	N1	122.6(2)	124.1	1.5	123.4(2)	124.0	0.6

geometrical parameters of the synthesized compounds are comparable to each other and both have monoclinic structures. Smaller N—C11 bond length as compared to N—C12 confirms the marked double bond character in the N—C11 bond.

Intramolecular hydrogen bonding is possible in both molecules between H atom of hydroxyl group and N atom in enolic as well zwitterionic forms (Table 3). The molecules have non-planar geometry as revealed by the torsional angles. The aromatic rings are not in the form of regular hexagons due the attached moieties. Two kinds of non-covalent interactions, {[C7···Br1 = 3.311 Å and H13···O1 = 2.482 Å] and [Cl1···C7 = 3.323 Å and H13···O1 = 2.481 Å]} offer 2D supramolecular structures to the compounds. The molecules are arranged in a manner to produce rectangular cavities of dimension *ca.* 10.249 × 6.564 Å and 15.434 × 6.680 Å (Fig. 2A and B). Such microporous structures are expected to find applications in separation and purification science, host–guest chemistry, gases storage and catalysis.

Electronic absorption spectroscopy

Electronic absorption spectra of BPIMN and CPIMN depicted in Fig. 3 shows five bands at 226, 318, 363, 441 and 460 nm in ethanol. In case of CPIMN, the band at 226 nm shifts to 223 nm. The band at 226 and 223 nm exhibit maximum absorbance with molar extinction coefficient, ε of 3.9×10^4 and 4.2×10^4 M^{-1} cm^{-1} for BPIMN and CPIMN respectively. The intense band at 226 nm and 223 nm are thought to be due to aromatic rings present in the structures involving π–π^* transitions. Less intense bands at 318 nm are probably due to π–π^* transitions of —C=N group. As intramolecular hydrogen bonding is possible between —C=N and —OH (Scheme 3) so there is a decrease of π–π^* energy in comparison to first band. Peaks in the range of 363–460 nm include n–π^* transitions due to —C=N and —C=O moieties. The location of these peaks at longer wavelengths can be explained in terms of electron releasing nature of —OH and —N=C groups. The existence of BPIMN and CPIMN in zwitterionic forms as evidenced by electrochemical investigations, crystal studies and theoretical energy optimization (Scheme 4) results in the separation of peaks in the range of 360–460 nm. Literature survey reveals the formation of zwitterionic forms in the crystal structure of ortho-hydroxy Schiff bases [26]. Normally, such zwitterionic forms occur by a proton transfer from orthohydroxy group to the nitrogen lone pair in the phenol-imine form through a six membered transition state. Neutralization of the negative and positive charges in the zwitterionic form results in the formation of neutral keto-amine form.

Fig. 4 shows the electronic absorption spectra of 20 μM BPIMN and CPIMN in acidic and basic media. The results obtained from the spectra recorded in different pH media helped in the determination of pK_a of the —OH group present in the molecule. BPIMN showed an intense doublet at 231–247 nm in the pH range 4–12, while the intense band of CPIMN moved to much shorter wavelengths with the appearance of less intense band at 245 nm. This spectral behavior can be explained on the basis of electronegativity values of chlorine and bromine atoms. Chlorine being more electronegative deactivates benzene ring so imparts hypsochromic shift to the first band along with hypochromic effect on the second band,

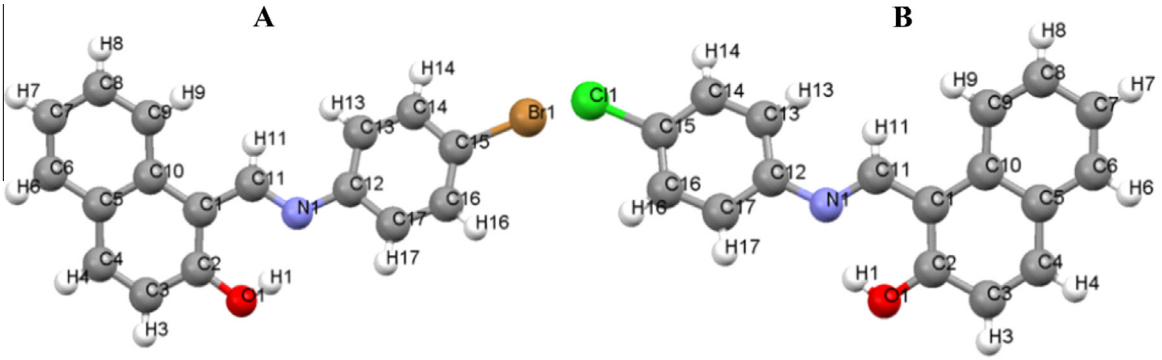

Fig. 1. Ball and stick diagrams of BPIMN (A) and CPIMN (B).

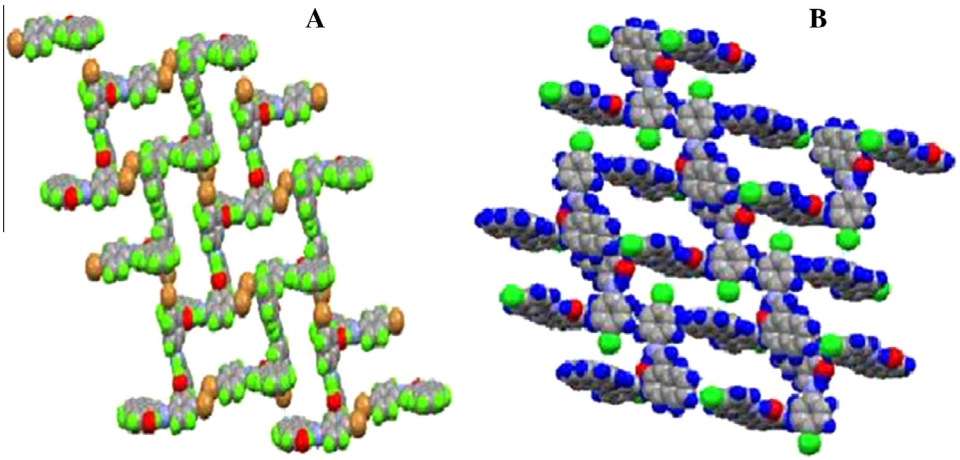

Fig. 2. (A) 2D microporous structure of the compound BPIMN mediated by C7···Br1 = 3.311 Å and H13···O1 = 2.482 Å and (B) 2D microporous structure of the compound CPIMN mediated by Cl1···C7 = 3.323 Å and H13···O1 = 2.481 Å.

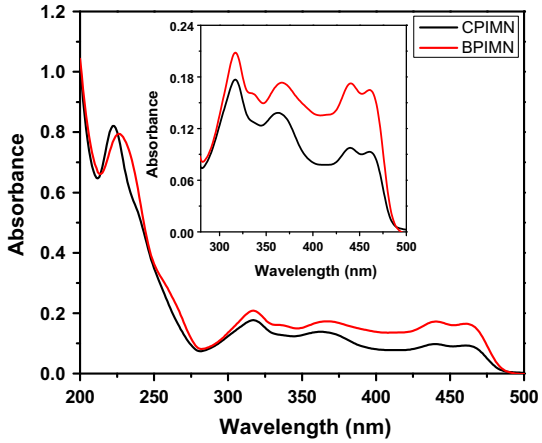

Fig. 3. UV–Vis spectra of 20 μM BPIMN and CPIMN in ethanol.

while bromine being less electronegative imparts bathochromic and hyperchromic shifts to the second band, hence, both bands of BPIMN appear as doublet.

In strongly acidic medium, hypsochromic effect occurs in the most intense band due to protonation of —OH and —C=N groups. These moieties gain positive charge after proton capture and hence, cause to deactivate the aromatic ring. This effect can also be confirmed by the disappearance of band at 318 nm in CPIMN spectra due to —C=N and hypochromic effect in the third band. In pH 6.0 and 8.0, probability of protonation reduces, therefore; both these molecules show well resolved bands at 440 and 460 nm. Further increase in pH results in more blue shift of intense band toward the UV region. With the rise in pH of the medium, the peak at 245 nm (due to π–π^* transitions) intensifies, the band at 318 nm decays and a new intense peak corresponding to n–π^* transitions appears at 397 nm. These peculiar spectral characteristics can be explained by the deprotonation of —C—OH group which gets converted to —C=O in alkaline medium and gives new peaks at 245 and 397 nm. Moreover, BPIMN shows three isosbestic points at 239, 299 and 337 nm, indicating its existence in three different forms. pK_a of BPIMN and CPIMN with values 9.2 and 6.7 were calculated from the plots of absorbance *versus* pH.

Cyclic voltammetry

The cyclic voltammetry of 1 mM solutions of BPIMN and CPIMN was performed at a scan rate of 100 mV s^{-1} in medium of pH 7.0 using GCE in the potential range of −1.6 to +1.5 V. CPIMN registered one oxidation peak at +0.725 V and three reduction peaks at −0.92, −1.24 and −1.48 V, while BPIMN oxidized at +0.710 V. Voltammograms of both the compounds were recorded in different potential windows in order to ensure the dependent or independent nature

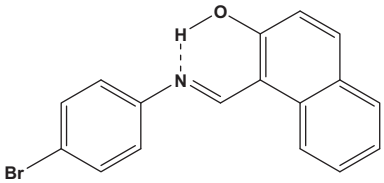

BPIMN

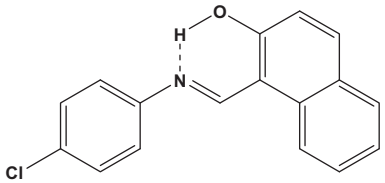

CPIMN

Scheme 3. Intramolecular hydrogen bonding in BPIMN and CPIMN.

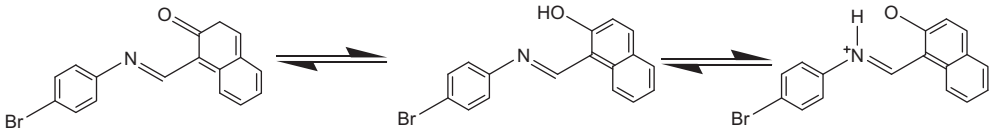

Scheme 4. Tautomeric forms of BPIMN.

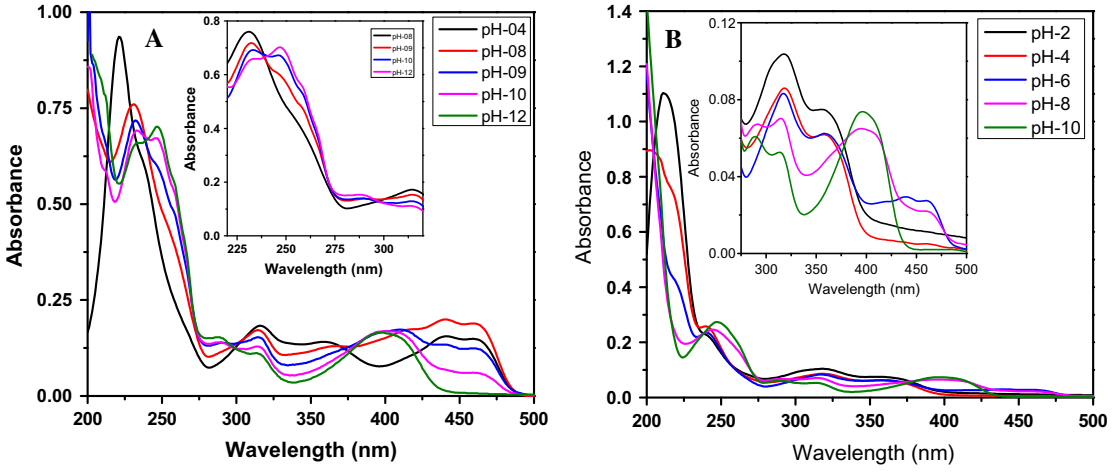

Fig. 4. Electronic absorption spectra of 20 μM BPIMN (A) and CPIMN (B) recorded in different pH media.

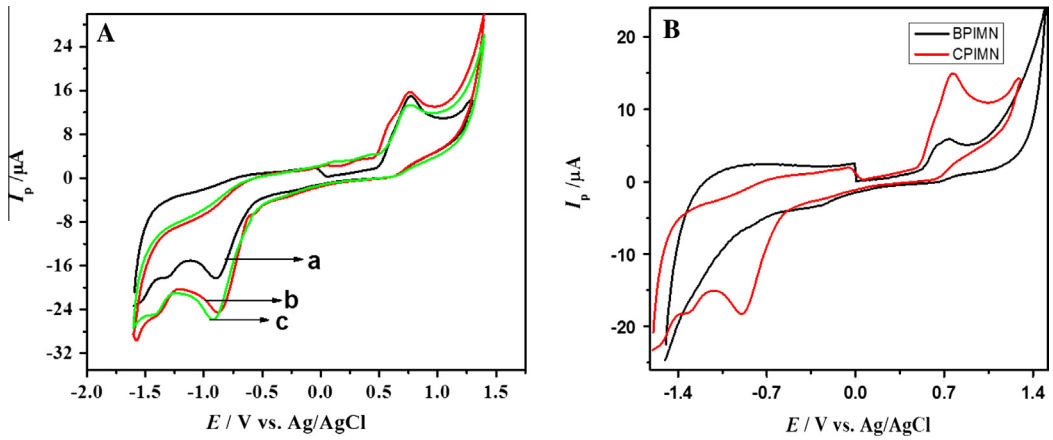

Fig. 5. (A) The CVs of CPIMN recorded at 100 mV s^{-1} starting from 0 V (a) −0.6 V (b) and −1.4 V (c) with 1 mM concentration of analyte in 50% ethanol and 50% BR buffer of pH-7, (B) voltammogram of BPIMN and CPIMN obtained under same conditions.

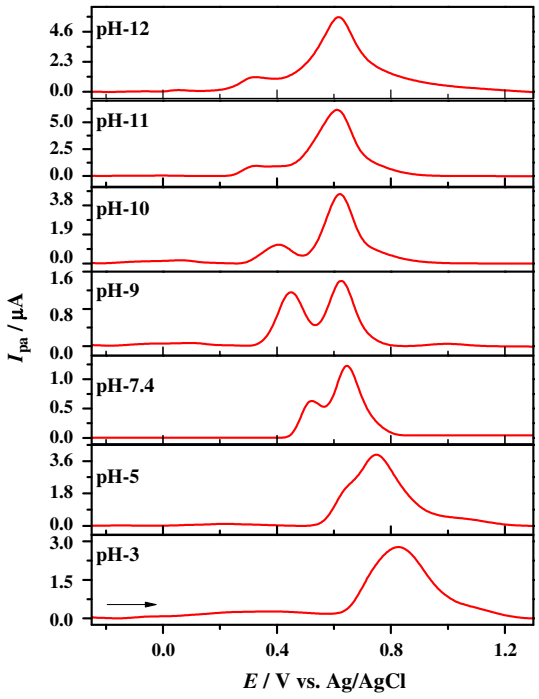

Fig. 6. Differential pulse voltammograms for oxidation of CPIMN at 10 mV s^{-1} in 50% ethanol and 50% BR buffers of wide pH range used as supporting electrolyte.

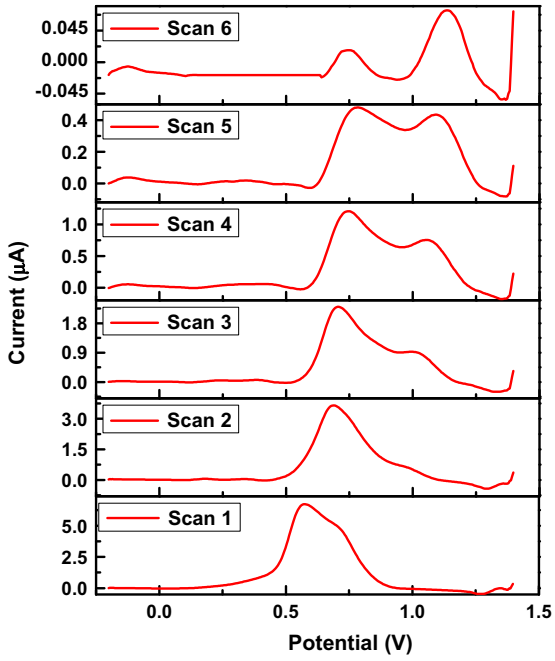

Fig. 7. Multiple scan SWVs of 1 mM CPIMN recorded at 100 mV s^{-1} in 50% ethanol and 50% BR buffer of pH-7, used as supporting electrolyte.

of the peaks (Fig. 5). Cathodic and anodic peaks of CPIMN were found independent of each other and hence, generated by separate reducible and oxidizable moieties of the compound.

A remarkable feature of these voltammograms is that the Schiff base having chloro group has three reduction signals while bromo containing Schiff base has no prominent peak in the cathodic region. This clear voltammetric distinction can be related to the more electronegative character of chloro group in encouraging the N of azomethine to donate its lone pair of electrons toward the phenyl ring thus rendering the C=N group to reduce in the negative potential domain of GCE. In case of comparatively less electron withdrawing ability of bromo group, the azomethine functionality may remain electron rich hence no signals of reduction appear at the GCE.

In order to investigate the adsorption of CPIMN at the surface of working electrode, consecutive scans were recorded without cleaning the electrode. A reasonably small decrease in peak current indicated slight adsorption of the analyte. The plot between log of scan rate and log of peak current evidenced the redox processes to be mainly controlled by diffusion and slightly by adsorption. Moreover, there is indication of the appearance of another oxidation peak at higher positive potential in the second scan which gets more prominent with further scans. Multiple SW voltammograms (see Section 'Square wave voltammetry') offered more clear evidence of the appearance of this second peak due to more sensitivity.

Differential pulse voltammetry

DPVs of 1 mM BPIMN and CPIMN were obtained in a broad pH range (2–12) in order to ensure the involvement of proton during electron transfer processes. The width at half peak height ($W/2$) of all oxidation and reduction peaks were determined at different pH values. In case of CPIMN, the oxidation signal was broad in the pH range 3–8 due to two overlapping peaks, which split into

two well defined separate peaks of 88 mV half peak heights at pH 9.0 as shown in Fig. 6.

These $W/2$ values are very close to the theoretical value (90.4 mV) of one electron transfer process [27,28]. BPIMN showed almost the same behavior with peak splitting occurring at pH-8.0. Thus, in the electrochemical processes of these Schiff bases, one electron is involved in all signals as confirmed from their $W/2$ values. The peak potentials shifted with change in pH of the medium. E_{pa1} as a function of pH with a slope of 55 mV per unit pH (closer to 59 mV theoretical value) demonstrated the involvement of one electron and one proton in the first oxidation step [29]. The participation of the same number of electrons and protons in the second oxidation process was shown by the of 57 mV per unit pH slope E_{pa2} *versus* pH plot [30].

Square wave voltammetry

Square wave voltammograms of 1 mM CPIMN were obtained in the pH interval of 3–12 at a scan rate of 100 mV s^{-1}. Like CV, SWV showed irreversible nature of oxidation and reduction processes of CPIMN. Five successive potential scans recorded without cleaning the working electrode surface are displayed in Fig. 7. An examination of the voltammograms shows that a new peak appears at more positive potential in the second scan, which becomes more prominent in the third and fourth scans, while height of the original peak diminishes in later scans.

Redox mechanism of BPIMN and CPIMN

1-((4-Chlorophenylimino) methyl) naphthalen-2-ol exists in enolic and zwitterionic forms as confirmed by computational and FTIR studies. The oxidation of CPIMN gave a broad oxidation peak in acidic medium, which split into two distinct peaks in basic medium. This is because when the medium is acidic, proton combines with negatively charged oxygen of zwitterionic form and thus the enolic form of the compound exists in acidic medium. The half peak width values of both peaks indicated the transfer of one electron each. The oxidation of hydroxyl part occurs by the loss of one electron and one proton below pH 9. This peak becomes pH independent above pH 9 and hence, abstraction of one electron occurs without involvement of proton in highly alkaline conditions. The appearance of another oxidation peak at pH $\geqslant$ 9 can be related to the presence of zwitterionic form of CPIMN. The oxidation corresponding to this peak occurs by the loss of one electron and one proton as witnessed by 88 mV half peak width and 57 mV pH^{-1} slope of E_p *versus* pH plot. The appearance of an extra peak in the SW voltammogram of CPIMN at more positive potential in 2nd and higher scans is due to the shifting of equilibrium toward enolic

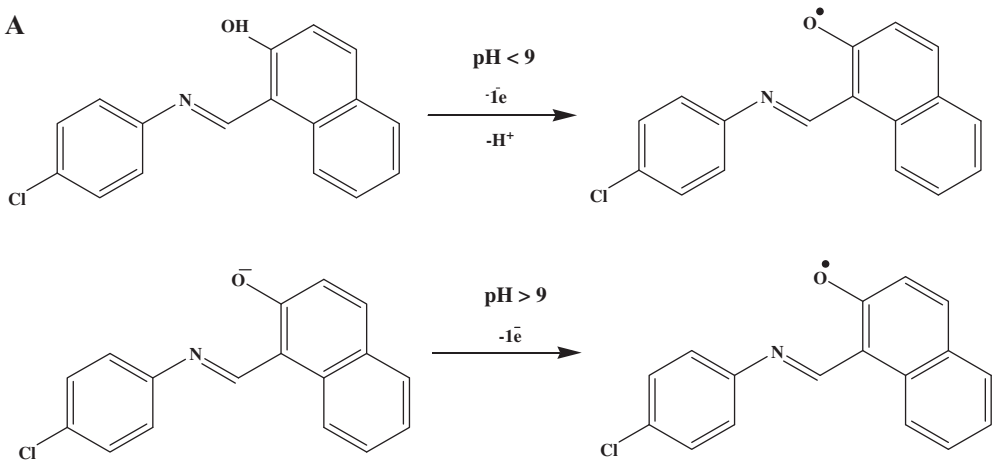

Scheme 5(A). Proposed oxidation mechanism of CPIMN corresponding to peak 1a.

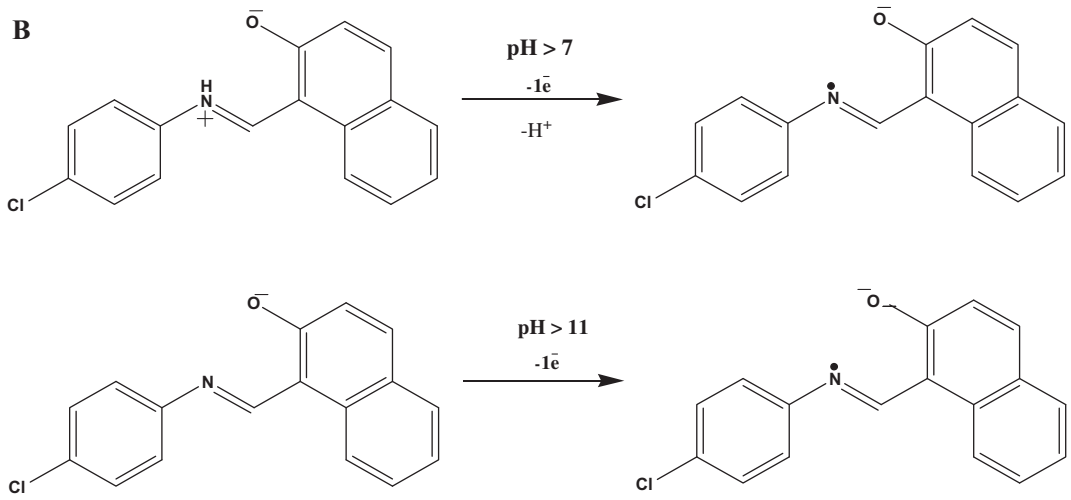

Scheme 5(B). Proposed oxidation mechanism of CPIMN corresponding to peak 2a.

Table 4
Selected parameters of BPIMN and CPIMN calculated by RB3LYP/3-21G set using DFT method in GAUSSIAN 03W package.

	BPIMN			CPIMN		
	Enol form	Keto form	Z.ionic form	Enol form	Keto form	Z.ionic form
Charge	0	0	0	0	0	0
Spin	Singlet	Singlet	Singlet	Singlet	Singlet	Singlet
Total energy (a.u.)	−3342.489	−3342.494	−3342.496	−1238.677	−1238.685	−1238.683
Dipole moment (D)	4.736	4.205	4.077	5.653	4.434	4.422
E_{HOMO} (a.u.)	−0.20541	−0.19498	−0.20082	−0.20912	−0.20418	−0.20395
E_{LUMO} (a.u.)	−0.06855	−0.06887	−0.07414	−0.07098	−0.07751	−0.07659
Point group	C1	C1	C1	C1	C1	C1

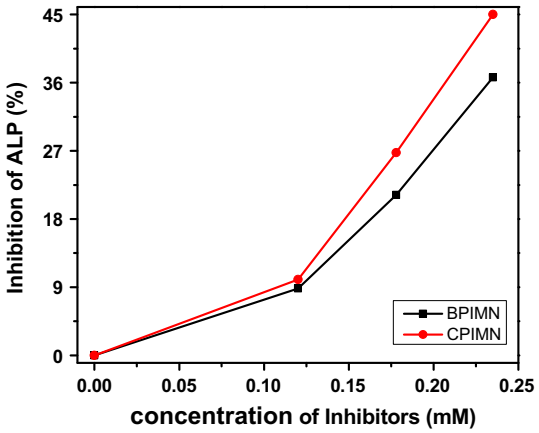

Fig. 8. Concentration dependent inhibition of alkaline phosphatase (ALPs) by BPIMN and CPIMN.

form. The proposed mechanism of CPIMN oxidation is presented in Scheme 5.

Computational study

The DFT optimized structures of the investigated compounds were obtained using 3-21G basis set [31]. Computational study of BPIMN and CPIMN was done to calculate the Mullikan charges, optimization energies, dipole moments, spin multiplicity and point groups of all three forms (see Table 4). The results reveal that keto and zwitterionic forms of both compounds are more stable than their enolic forms. From Mullikan Charge distribution values, it is obvious that oxygen atom of —OH group has the most negative charge which justify our attribution of electron abstraction from the same electropores.

Inhibition of ALP

Alkaline phosphatases (ALPs) occur widely in nature and found in many organisms [32]. In humans, it is produced in liver, bone, and placenta and normally present in high concentration in bile and growing bone. It is released into the blood during injury and during normal activities such as bone growth and pregnancy. The enzyme is termed alkaline phosphatase because it works under alkaline conditions, as opposed to acidic phosphatase [33]. With few exceptions, ALPs are homodimeric enzymes and each catalytic site contains three metal ions, i.e., two Zn and one Mg, necessary for enzymatic activity [34]. Increased level of ALP is indicative of hepatobiliary disease, osteoblastic activity and tumor formation [35]. Schiff bases are inhibitors of ALP and exert their inhibition effect by blocking the active sites of the enzyme. The results of our experiments reveal that chloro-substituted Schiff base inhibit the enzyme more effectively as compared to bromo-substituted Schiff base. ALPs were inhibited in a concentration-dependent manner (see Fig. 8); however, these Schiff bases were not able to completely inhibit the enzymes.

Conclusion

Two Schiff bases abbreviated as CPIMN and BPIMN were successfully synthesized and characterized by different analytical techniques. The redox and photometric behavior of the compounds was found to depend strongly on the pH of the medium. The existence of 1-((4-chlorophenylimino) methyl) naphthalen-2-ol in both enolic and zwitterionic forms was confirmed from FTIR, UV–Vis spectroscopy, computational, electrochemical and single crystal X-ray studies. Computational studies showed high negative charge density on oxygen atoms, thus, both Schiff bases are recommended as good ligands. Moreover, CPIMN was found to inhibit alkaline phosphatase enzyme more effectively than BPIMN.

Acknowledgments

The authors gratefully acknowledge the financial support of Higher Education Commission of Pakistan through Project No. 20-3070, Quaid-i-Azam University and the University of Toronto Canada. The authors would also like to extend their sincere appreciation to the Deanship of Scientific Research at King Saud University for funding this Research through the group Project No. RGP-VPP-345.

References

[1] M. Veith, S. Mathur, C. Mathur, Polyhedron 17 (1998) 1005–1034.
[2] W.B. Witkop, L.K. Ramachandran, Metabolism 13 (1964) 1016–1025.
[3] E.I. Solomon, M.D. Lowery, Science 259 (1993) 1575–1581.
[4] C. Gerdemann, C. Eicken, B. Krebs, Acc. Chem. Res. 35 (2002) 183–191.
[5] A.S. Kabeer, M. Baseer, N. Mote, Asian J. Chem. 13 (2001) 496–500.
[6] K. Bernardo, S. Leppard, A. Robert, G. Commenges, F. Dahan, B. Meunier, Inorg. Chem. 35 (2001) 387–396.
[7] A. Golcu, M. Tumer, H. Demirelli, R.A. Wheatley, Inorg. Chim. Acta 358 (2005) 1785–1797.
[8] A. Golcu, M. Dolaz, H. Demirelli, M. Diorak, S. Serin, Transition Met. Chem. 31 (2006) 658–665.
[9] E. Hadjoudis, M. Vittorakis, I. Moustakali-Mavridis, Tetrahedron 43 (1987) 1345–1360.
[10] G. Alpaslan, M. Macit, A. Erdonmez, O. Buyukgüngor, J. Mol. Struct. 997 (2011) 70–77.
[11] C.M. Metzler, A. Cahill, D.E. Metzler, J. Am. Chem. Soc. 102 (1980) 6075–6082.
[12] S. Alarcón, D. Pagani, J. Bacigalupo, A. Olivieri, J. Mol. Struct. 475 (1999) 233–240.
[13] P.S. Ray, G. Maulik, G.A. Cordis, A.A. Bertelli, A. Bertelli, D.K. Das, Free Radical Biol. Med. 27 (1999) 160–169.
[14] S. Kumar, D.N. Dhar, P. Saxena, J. Sci. Ind. Res. 68 (2009) 181–187.
[15] E.M. Hodnett, W.J. Dunn, J. Med. Chem. 15 (1972) 339–344.
[16] E. Naderi, M. Ehteshamzadeh, A. Jafari, M. Hosseini, Mater. Chem. Phys. 120 (2010) 134–141.
[17] S. Safak, B. Duran, A. Yurt, G. Turkoglu, Corros. Sci. 54 (2012) 251–259.
[18] M. Behpour, S.M. Ghoreishi, N. Mohammad, N. Behpour, M. Soltani, M. Salavati-Niasari, Corros. Sci. 52 (2010) 4046–4057.
[19] A.H. Kianfar, V. Sobhani, M. Dostani, M. Shamsipur, M. Roushani, Inorg. Chim. Acta 365 (2011) 108–112.
[20] A. Kianfar, S. Mohebbi, J. Iranian Chem. Soc. 4 (2007) 215–220.
[21] S. Riahi, S. Eynollahi, M. Ganjali, Int. J. Electrochem. Sci. 4 (2009) 1128–1137.

[22] G.K. Pierens, T. Venkatachalam, P.V. Bernhardt, M.J. Riley, D.C. Reutens, Aust. J. Chem. 65 (2012) 552–556.
[23] O.V. Dolomanov, L.J. Bourhis, R.J. Gildea, J.A. Howard, H. Puschmann, J. Appl. Crystallogr. 42 (2009) 339–341.
[24] X.L. Gao, L.P. Lu, M.L. Zhu, Acta Crystallogr. Sect. C: Cryst. Struct. Commun. 65 (2009) 123–127.
[25] M.R. Malik, V. Vasylyeva, K. Merz, N. Metzler-Nolte, M. Saleem, S. Ali, A.A. Isab, K.S. Munawar, Inorg. Chim. Acta 376 (2011) 207–211.
[26] H. Karabıyık, N. Ocak-Iskeleli, H. Petek, C. Albayrak, E. Agar, J. Mol. Struct. 873 (2008) 130–136.
[27] K. Ahmad, A.H. Shah, B. Adhikari, U.A. Rana, S. Noman-uddin, C. Vijayaratnam, N. Muhammad, S. Shujah, A. Rauf, H. Hussain, A. Badshah, R. Qureshi, H.B. Kraatz, A. Shah, RSC Adv. 4 (2014) 31657–31665.
[28] A. Munir, A. Shah, A.H. Shah, U.A. Rana, B. Adhikari, S.B. Khan, R. Qureshi, H.B. Kraatz, J. Electrochem. Soc. 161 (2014) H370–H374.
[29] S. Munir, A. Shah, U.A. Rana, I. Shakir, Z. Rehman, S.M. Shah, Aust. J. Chem. 67 (2014) 206–212.
[30] A. Shah, A. Ullah, A. Rauf, Z. Rehman, S. Shujah, S.M. Shah, A. Waseem, J. Electrochem. Soc. 160 (2013) H597–H603.
[31] B. Latha, S. Gunasekaran, S. Srinivasan, G.R. Ramkumaar, Spectrochim. Acta Part A: Mol. Biomol. Spectrosc. 132 (2014) 375–386.
[32] D.G. Herries, Biochem. Educ. 9 (1981) 76.
[33] L. Tamas, J. Huttova, I. Mistrik, G. Kogan, Chem. Pap. 56 (2002) 326–329.
[34] E.E. Kim, H.W. Wyckoff, Clin. Chim. Acta 186 (1990) 175–187.
[35] M.D.S. Shephard, M.J. Peake, J. Clin. Pathol. 39 (1986) 1025–1030.